Molecular Biology of the Cell
Vol. 20, 3918–3929, September 1, 2009

Identification of a Distal GLUT4 Trafficking Event Controlled by Actin Polymerization

Jamie A. Lopez,*† James G. Burchfield,*† Duncan H. Blair,* Katarina Mele,*‡ Yvonne Ng,* Pascal Vallotton,‡ David E. James,*§ and William E. Hughes*‖

*Diabetes and Obesity Research Program, The Garvan Institute of Medical Research, Sydney, NSW 2010, Australia; ‡CSIRO Mathematical and Information Sciences, Sydney, NSW 1670, Australia; §School of Biotechnology and Biomolecular Sciences, University of New South Wales, Sydney NSW 2052, Australia; and ‖Department of Medicine, St. Vincent's Hospital, University of New South Wales, Sydney, NSW 2010, Australia

Submitted March 5, 2009; Revised June 22, 2009; Accepted July 2, 2009
Monitoring Editor: Thomas F.J. Martin

The insulin-stimulated trafficking of GLUT4 to the plasma membrane in muscle and fat tissue constitutes a central process in blood glucose homeostasis. The tethering, docking, and fusion of GLUT4 vesicles with the plasma membrane (PM) represent the most distal steps in this pathway and have been recently shown to be key targets of insulin action. However, it remains unclear how insulin influences these processes to promote the insertion of the glucose transporter into the PM. In this study we have identified a previously uncharacterized role for cortical actin in the distal trafficking of GLUT4. Using high-frequency total internal reflection fluorescence microscopy (TIRFM) imaging, we show that insulin increases actin polymerization near the PM and that disruption of this process inhibited GLUT4 exocytosis. Using TIRFM in combination with probes that could distinguish between vesicle transport and fusion, we found that defective actin remodeling was accompanied by normal insulin-regulated accumulation of GLUT4 vesicles close to the PM, but the final exocytotic fusion step was impaired. These data clearly resolve multiple steps of the final stages of GLUT4 trafficking, demonstrating a crucial role for actin in the final stage of this process.

INTRODUCTION

The insulin-dependent uptake of glucose by adipose and muscle tissues is accomplished through the regulated trafficking of the GLUT4 glucose transporter to the plasma membrane (PM; Larance *et al.*, 2008; Zaid *et al.*, 2008). Within the cell GLUT4 is closely associated with several intracellular compartments including recycling endosomes, the *trans*-Golgi network, and tubulovesicular elements (Slot *et al.*, 1991). The tubulovesicular elements maintain a highly insulin-responsive GLUT4 compartment known as GLUT4 storage vesicles (GSVs) that are enriched in several polypeptides including GLUT4, the insulin-responsive amino-peptidase (IRAP), the Rab GAP TBC1D4/AS160 and vesicle associated membrane proteins (VAMP; Larance *et al.*, 2005). The insulin-stimulated exocytosis of GLUT4 is achieved through the initiation of a signaling cascade that regulates the physical trafficking or translocation of GSVs to the PM. These signaling events have been extensively characterized (Taniguchi *et al.*, 2006) and involve the recruitment and activation of phosphoinositide 3-kinase (PI3-K) and Akt/PKB on the inner surface of the PM and subsequent phosphorylation of downstream substrates including TBC1D4 that promote GLUT4 vesicle movement toward the PM, where they subsequently dock and fuse. The docking and fusion of GLUT4 vesicles is thought to involve a regulated interaction between membrane bound SNARE (soluble *N*-ethylmaleimide–sensitive factor attachment protein) proteins consisting of the *v*-SNARE VAMP2 and plasma membrane bound *t*-SNAREs Syntaxin4 and SNAP23 (synaptosome-associated protein of 23 kDa; Larance *et al.*, 2008). In addition, a number of SNARE regulatory proteins (Latham *et al.*, 2006; Bao *et al.*, 2008), as well as a tethering complex (Inoue *et al.*, 2003), have been identified that are thought to participate in these steps. Although some of the molecular players that mediate GLUT4 trafficking have been identified, in general these distal trafficking steps remain largely uncharacterized.

Recently, total internal reflection fluorescence microscopy (TIRFM) has been used to visualize GLUT4 vesicle-trafficking events close to the PM (Li *et al.*, 2004; Lizunov *et al.*, 2005; Bai *et al.*, 2007; Huang *et al.*, 2007). The advantage of this technique is that it enables selective detection of fluorescently labeled proteins within ~200 nm of the cell surface (Axelrod, 2008; Burchfield *et al.*, 2009). Work from several independent groups suggests that the major action of insulin on GLUT4 exocytosis is on vesicle tethering, docking, and/or fusion at the PM (Lizunov *et al.*, 2005; Bai *et al.*, 2007; Huang *et al.*, 2007). In the basal state GLUT4-enhanced green fluorescent protein (eGFP) vesicles can be visualized approaching the PM and tethering/docking, but the rate of GLUT4 vesicle fusion with the cell surface remains low. Lizunov *et al.* (2005) showed in rat adipocytes that one of the primary actions of insulin was to capture or tether vesicles at the PM to promote vesicle fusion. Two subsequent studies showed that insulin promotes GLUT4 membrane insertion by decreasing the vesicle docking rate and more importantly increasing the rate of vesicle fusion (Bai *et al.*, 2007; Huang *et al.*, 2007). However, the molecular regulation of these steps remains poorly described.

This article was published online ahead of print in *MBC in Press* (http://www.molbiolcell.org/cgi/doi/10.1091/mbc.E09–03–0187) on July 15, 2009.

† These authors contributed equally to this work.

Address correspondence to: David E. James (d.james@garvan.org.au) or William E. Hughes (w.hughes@garvan.org.au).

The cytoskeleton plays an important role in GLUT4 exocytosis with both microtubules and actin filaments being implicated (Omata *et al.*, 2000; Fletcher *et al.*, 2001; Kanzaki and Pessin, 2001; Olson *et al.*, 2001; Patki *et al.*, 2001). Microtubules direct the transport of GLUT4 vesicles to the cell cortex, and this process has been shown to involve the kinesin motor protein KIF5B (Semiz *et al.*, 2003). Furthermore, several insulin-regulated proteins have been identified that control actin dynamics to influence GLUT4 exocytosis, for example, TC10 (Kanzaki *et al.*, 2002), N-WASP (Jiang *et al.*, 2002), and Fodrin (Liu *et al.*, 2006). The unconventional myosin Myo1c was also shown to play a significant role in GLUT4 trafficking (Bose *et al.*, 2004) and recently was identified as a downstream substrate of insulin signaling (Yip *et al.*, 2008). Interestingly studies by Czech and colleagues have placed Myo1c function at a step close to GLUT4 vesicle fusion (Bose *et al.*, 2004). Emerging from these observations is a model where GLUT4 vesicles traffic along microtubules from the perinuclear area to the cortex. Here they may exchange with cortical actin although the details of this are not well described.

Our goal in the present study was to delineate the role of actin in GLUT4 trafficking in adipocytes. Insulin was shown to increase cortical actin polymerization and remodeling while increasing the rate at which GLUT4 vesicles fuse with the PM. Disruption of the cortical actin network was shown to drastically inhibit the GLUT4 vesicle fusion rate, resulting in less GLUT4 incorporation into the PM. The accumulation of vesicles under the PM in response to insulin was dependent on an intact PI3-K/Akt pathway but not a cortical actin network. We propose that the polymerization and remodeling of cortical actin at the PM is a necessary and rate-limiting step for GLUT4 vesicle fusion.

MATERIALS AND METHODS

Reagents

DMEM cell culture medium, antibiotics, newborn calf serum, enhanceFX, and Matrigel were from Invitrogen (Carlsbad, CA). Fetal calf serum was from ThermoTrace (Melbourne, Australia). Antibodies used were obtained as follows: rabbit anti-Akt(pan), rabbit anti-pAkt(S473), rabbit anti-pS6K(T389), rabbit anti-pGSKβ(S9), rabbit monoclonal phosho-Akt-substrate antibodies (Cell Signaling Technology, Danvers, MA), mouse anti-hemagglutinin (HA) antibodies (Covance Research Products, Berkley, CA), mouse anti-α-tubulin antibody (Sigma-Aldrich, St. Louis, MO), anti-rabbit and anti-mouse horseradish peroxidase–conjugated secondary antibodies (GE Healthcare; Uppsala, Sweden), anti-rabbit and anti-mouse infrared-dye–conjugated secondary antibodies (Rockland Immunochemicals, Gilbertsville, PA), and anti-mouse Alexa-Fluor-488–conjugated secondary antibodies (Molecular Probes, Leiden, The Netherlands). The sheep anti-pTBC1D4(T642) antibody and the Akt inhibitor Akti-1/2 was obtained from P. Shepherd (Symansis, Auckland, NZ). All other reagents were obtained as follows: tetramethylrhodamine isothiocyanate (TRITC)-conjugated phalloidin (Sigma), transferrin-Alexa 488 (Molecular Probes). The IRAP-TfR chimera (VpTfR) was a gift from T. McGraw (Weill Cornell Medical College, New York). The GLUT4-eGFP and IRAP-pHluorin plasmids were a gift from T. Xu (Institute of Biophysics, Chinese Academy of Sciences, Beijing, China). All chemicals were obtained from Sigma-Aldrich.

Cell Culture and Electroporation

3T3-L1 fibroblasts were obtained from the Howard Green laboratory (Boston, MA). Cells were cultured and differentiated into adipocytes as previously described (Larance *et al.*, 2005). Adipocytes were electroporated at 5–7 d after differentiation with GLUT4-eGFP or IRAP-pHluorin plasmids as previously described (Stockli *et al.*, 2008). HA-GLUT4-pBABEpuro and IRAP-TfR-pBABEpuro retrovirus was prepared and used to infect 3T3-L1 fibroblasts as previously described (Shewan *et al.*, 2003).

Preparation of Matrigel-coated Coverslips

Glass coverslips, 42 mm, were incubated at room temperature for 120 min with a 1:50 dilution of Matrigel in ice-cold DMEM. Coverslips were subsequently washed twice with PBS and used as required.

Pharmacological Treatments

All drugs or inhibitors were solubilized in DMSO before their use. An equivalent concentration of DMSO was used as the vehicle control in all experiments. Cells were serum-starved for 120 min before insulin (100 nM) stimulation. Cells were incubated with drugs or inhibitors as follows: for latrunculin experiments cells were incubated with 10 μM latrunculin B (Lat-B) 60 min before insulin stimulation, for BAPTA-AM experiments cells were incubated with 50 μM BAPTA-AM 10 min before insulin stimulation, for wortmannin experiments cells were incubated with 100 nM wortmannin 15 min before insulin stimulation, and for the Akt inhibitor treatments cells were incubated with 10 μM of Akti 1/2 15 min before insulin stimulation.

Confocal Laser-scanning Microscopy

Cells were washed three times in cold PBS, fixed with 3% (vol/vol) paraformaldehyde in PBS, blocked in 2% (wt/vol) BSA containing 0.1% (wt/vol) saponin in PBS (or no saponin for surface labeling experiments), and incubated with primary antibodies and fluorescently conjugated secondary antibodies as indicated. Tf-Alexa-488 surface labeling was described previously (Ng *et al.*, 2008). Slides were examined using a Leica SP2 laser scanning confocal microscope (Leica Microsystems, Wetzlar, Germany). Cytoskeletal elements were visualized and analyzed using Imaris (Bitplane, Zurich, Switzerland).

Live Cell TIRF Microscopy

Coverslips were mounted in a heated stage microscope insert 'P' (Pecon, Waltham, MA) on an Axiovert 200M (Zeiss, Jena, Germany) equipped with a large incubator (XL, Pecon) maintained at 37°C. Suitably transfected cells were identified by fluorescence using a 100× objective (NA 1.4 Alpha-Plan, Zeiss), and TIRFM was performed using a 488-nm laser introduced into the excitation light path (488/5 nm) through the TIRF-slider (Zeiss) and appropriately angled to image ~250 nm into cells as previously described (Falasca *et al.*, 2007). Fluorescence (525/25 nm) was detected using an iXon DU-888D EMCCD camera (Andor Technology, South Windsor, CT), and images were taken at a rate of ~10 frames/s.

Fixed Cell TIRF-M

Cells on 42-mm coverslips were fixed in 3.8% (vol/vol) paraformaldehyde, permeabilized with 0.1% (wt/vol) saponin in PBS, and blocked with enhanceFX. Cells were stained for 20 min with TRITC-phalloidin in PBS containing 0.1% (wt/vol) saponin, according to manufacturer's recommendations. Cells were washed six times with PBS containing 0.1% (wt/vol) saponin. Cells were imaged in PBS containing 5% (vol/vol) glycerol and 2.5% (vol/vol) DAPKO using the microscopy setup described above. Images were captured using a Zeiss Axiocam MRm. To avoid user bias, cells were randomly selected by bright-field illumination before TIRF imaging.

HA-GLUT4 Translocation Assays

3T3-L1 fibroblasts were infected with HA-GLUT4 retrovirus and differentiated in 96-well plates. Cells were incubated in the absence or presence of insulin (100 nM) for 20 min. The HA-GLUT4 quantitative fluorescence assay was performed as previously described (Govers *et al.*, 2004).

Signaling Experiments

3T3-L1 adipocytes were serum-starved and incubated in the absence or presence of insulin (100 nM) for 30 min. Cells were washed three times in cold PBS, scraped into cold HES buffer (20 mM HEPES, 10 m EDTA, and 250 mM sucrose, pH 7.4) containing 2% (vol/vol) SDS, containing Complete protease inhibitor (Roche, Indianapolis, IN) and phosphatase inhibitors (2 mM sodium orthovanadate, 1 mM pyrophosphate, 1 mM ammonium molybdate, and 10 mM sodium fluoride). Lysates were centrifuged at 16,200 × *g* for 10 min, and supernatants were analyzed by SDS-PAGE and immunoblotting with antibodies as indicated.

Quantitative Analysis of Fusion Events Using TIRF Explorer

Fusion event candidates were detected using the TIRF Explorer software (Mele *et al.*, 2009). Briefly, regions showing rapid changes in intensity were identified from the time-lapse sequences and assembled in a 3D stack, and the absolute difference between consecutive frames was calculated. Regions that are more variable have higher values and consist mainly of fusion events and moving vesicles. Connected regions representing candidate events were then extracted from the highly variable parts of the 3D volume, and each candidate was manually inspected using TIRF Explorer and ImageJ (http://rsb.info.nih.gov/ij/; NIH, Bethesda, MD) to confirm positive fusion events.

Analysis of Vesicle Accumulation

Average projections were generated from the frames equivalent to 2-min intervals of TIRFM movies from latrunculin-treated cells using ImageJ. Structures that remained stationary during this 2-min interval appeared as spots, whereas moving structures appeared as part of the blurred background. Vesicles were detected and quantitated using the Spots function in Imaris

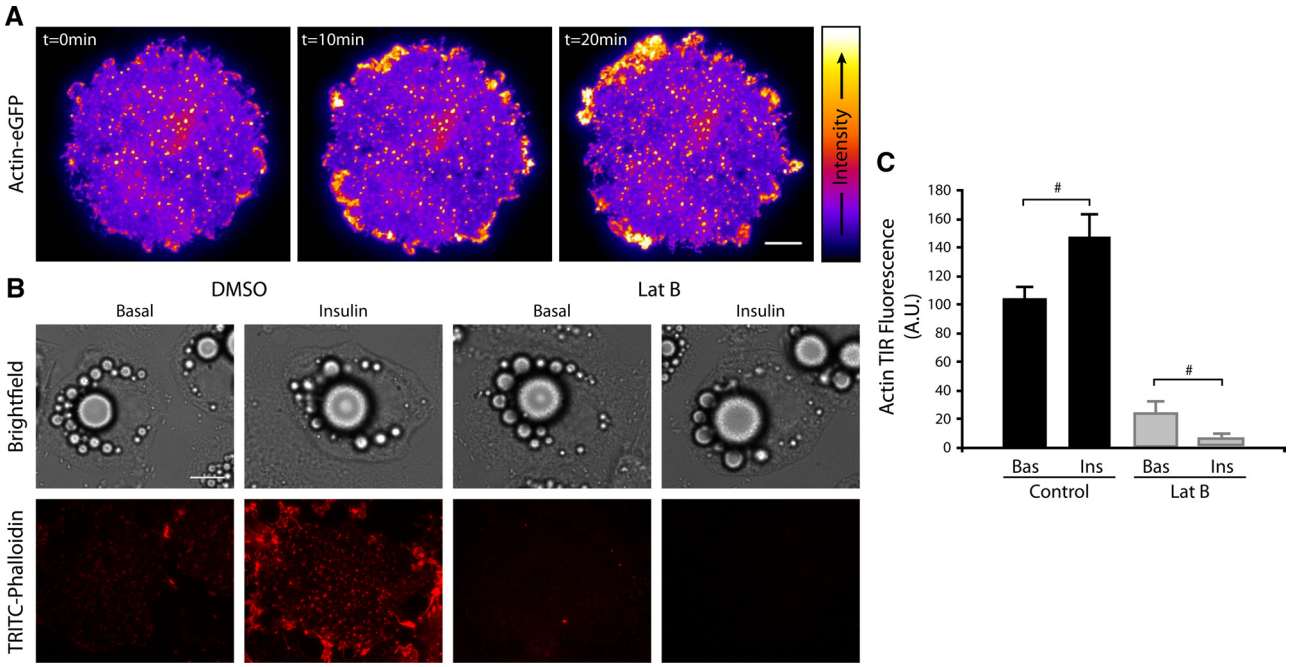

Figure 1. Insulin induces cortical actin remodeling in adipocytes as shown by TIRFM. Actin-eGFP expressing 3T3-L1 adipocytes were serum-starved for 120 min before imaging by TIRFM at 10 Hz for 2 min before stimulation with 100 nM insulin (at t = 0) and then were imaged for a further 20 min. (A) Representative images are shown from the time course. (B) 3T3-L1 adipocytes were serum-starved for 120 min and treated with DMSO ± 10 μM Lat-B for 1 h. Cells were then either unstimulated (Basal) or stimulated with 100 nM insulin (Insulin) for 30 min at 37°C, fixed, and labeled with TRITC-phalloidin then imaged by TIRFM. Representative images are shown. (C) The mean fluorescence of cells from three separate experiments are shown; # $p < 0.05$. Scale bar, (A and B) 10 μm.

(Bitplane). Background structures that were present for the entire movie were excluded from the analysis.

Statistical Analyses

Statistical analyses were performed with the use of statistical software package GraphPad Prism 4.03 (San Diego, CA) or using the basic statistical algorithms in Microsoft Office Excel 2003 (Redmond, WA). Data are presented as the mean ± SEM unless otherwise stated. Comparisons between two groups were performed using an independent two-sample *t* test. Comparisons between multiple groups were made using two-way ANOVA with Bonferroni post hoc tests to determine which sample pairs were significantly different.

RESULTS

Insulin Induces Cortical Actin Remodeling in Adipocytes

To investigate the role actin may have in regulating GLUT4 exocytosis in adipocytes, we first undertook a number of approaches to investigate the role insulin plays in regulating cortical actin structure. Insulin has been reported to promote the polymerization of actin in adipocytes (Kanzaki and Pessin, 2001), although changes specifically associated with the cortical actin or the PM have not been previously described. We used TIRFM to image changes in actin associated with the PM in response to insulin stimulation (Figure 1). 3T3-L1 adipocytes expressing actin-eGFP were imaged by live cell TIRFM before and after treatment with 100 nM insulin. Insulin treatment increased the dynamic remodeling of cortical actin including membrane puncta (Figure 1A and Supplementary Material, Movie 1), as well as increasing lamellipodia formation and stimulating an enrichment of actin in membrane ruffles consistent with observations in other cell types (Nobes and Hall, 1995; Figure 1A and Supplementary Material, Movie 1 and Supplementary Figure 1). This insulin-induced increase in polymerized cortical actin and associated puncta is particularly evident in TRITC-phalloidin stained cells treated with or without insulin imaged by TIRFM (Figure 1, B and C).

To further characterize the role of this insulin-dependent dynamic cortical actin, we used latrunculin B (Lat-B) to disrupt the actin cytoskeleton in 3T3-L1 adipocytes. Lat-B is a toxin derived from the Red Sea sponge (Spector *et al.*, 1983), and unlike other actin-disrupting agents such as cytochalasins, Lat-B has a specific inhibitory effect on actin polymerization. Lat-B sequesters the monomeric form of actin, and conformational changes induced by its binding are proposed to prevent subsequent polymerization (Morton *et al.*, 2000). Treatment of adipocytes with 10 μM Lat-B for 30 min resulted in a near complete disruption of cortical actin imaged by TIRFM compared with DMSO-treated control cells ($p < 0.001$; Figure 1, B and C). In the presence of insulin the rate of actin loss is increased by Lat-B treatment (Figure 1, B and C). Given the rate of Lat-B-induced cortical actin loss is proportional to the rate of actin turnover, this observation demonstrates that insulin not only increases the amount of polymerized actin but also increases the rate of actin remodeling.

We also examined TRITC-phalloidin stained cells treated with or without insulin by confocal microscopy (Figure 2). In reconstructions of TRITC-phalloidin–stained cells the increase in polymerized actin in response to insulin and the inhibitory effect of Lat-B are also evident confirming our observations made using TIRFM (Figure 2, A and C). In contrast to actin, tubulin labeling in 3T3-L1 adipocytes revealed a dense network of microtubules distributed throughout the cell, which was unaffected by Lat-B treatment (Figure 2, B and D). Thus, our imaging demonstrates that insulin induces cortical actin reorganization and that Lat-B treatment can be used to efficiently disrupt the

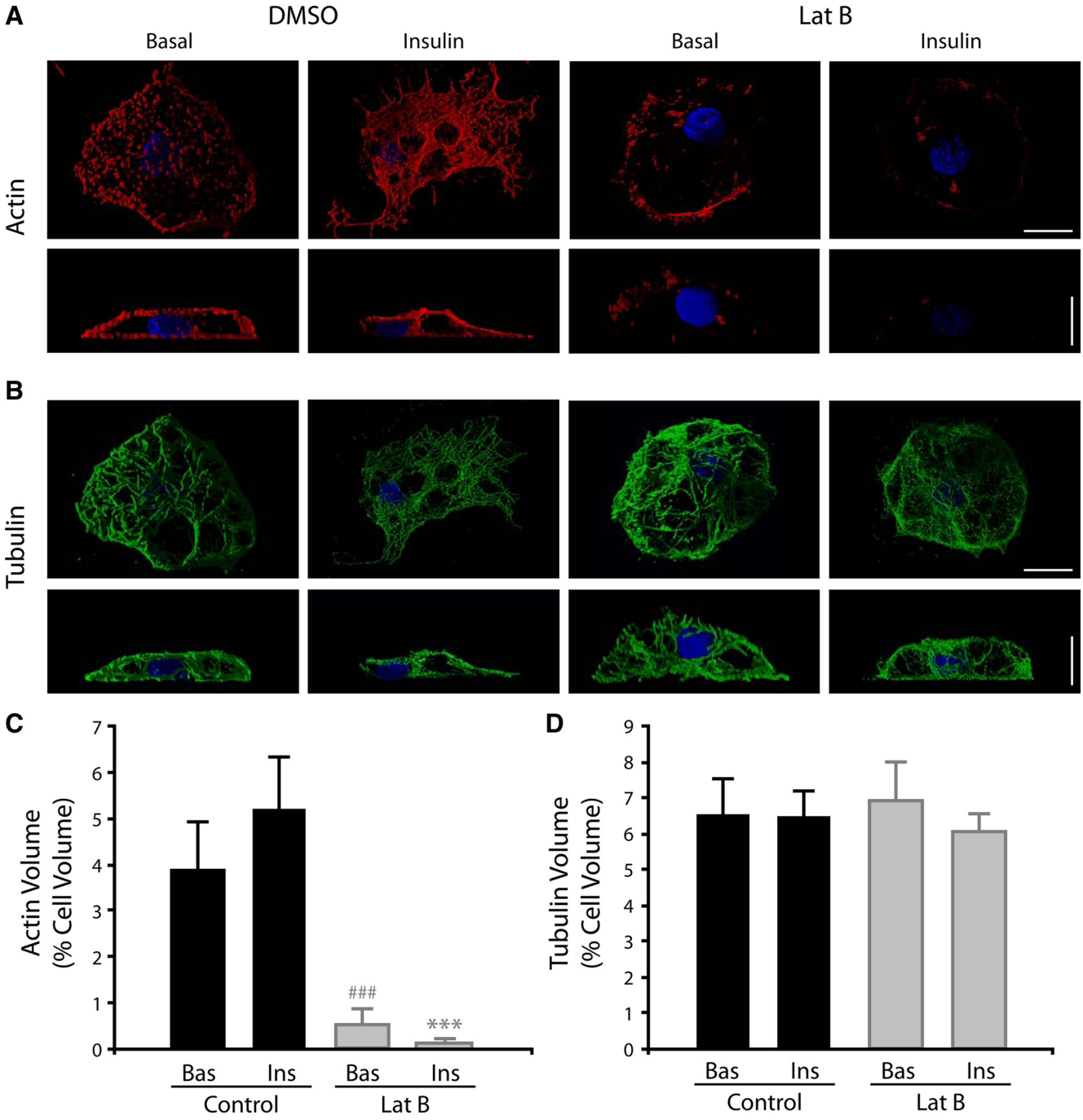

Figure 2. Insulin induces cortical actin remodeling in adipocytes as shown by confocal microscopy. 3T3-L1 adipocytes were serum starved for 120 min and treated with DMSO ± 10 μM Lat-B for 1 h. Cells were then either unstimulated (Basal) or stimulated with 100 nM insulin (Insulin) for 30 min at 37°C and fixed labeled, and the entire cell volume was imaged by confocal microscopy. Images shown are 3D shadow renderings of 120 confocal z-sections. F-actin staining with TRITC-phalloidin is shown red (A) and with tubulin (mouse anti-tubulin) is shown in green (B). DAPI staining is shown in blue. Scale bars, (A and B) 10 μm. The mean volumes of actin (C) and tubulin (D) expressed as a percentage of the total cell volume are show (n = 3 cells).

cortical actin network while leaving the microtubular network intact.

Disruption of Actin Remodeling Impairs Delivery of GLUT4 to the Plasma Membrane

To assess the effects of disrupting cortical actin remodeling on GLUT4 exocytosis, we examined the cellular distribution of a HA-GLUT4 reporter in adipocytes treated with and without insulin or Lat-B (Figure 3). The HA epitope is present in the first exofacial loop of the GLUT4 molecule and therefore surface HA antibody labeling can be used to assess GLUT4 incorporated into the PM. Insulin promoted the appearance of HA-GLUT4 at the cell surface, as seen by characteristic "rims" (Figure 3A), similar to those previously

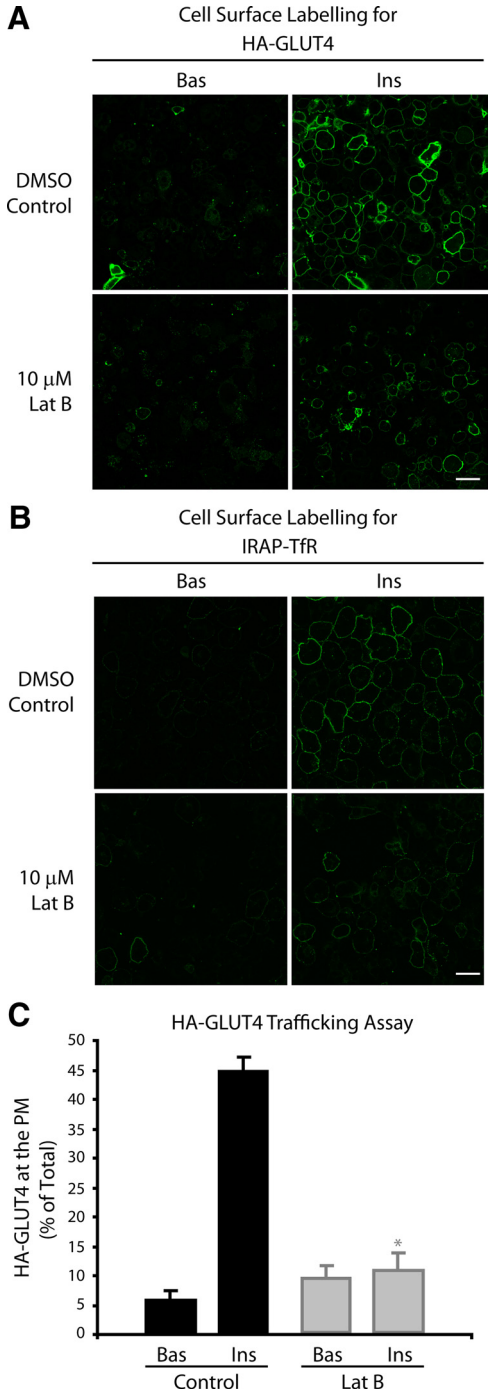

Figure 3. Disruption of actin remodeling impairs delivery of GLUT4 to the PM. (A) HA-GLUT4–expressing adipocytes were serum starved for 120 min and treated with DMSO ± 10 μM Lat-B for 1 h. Cells were then either unstimulated (Bas) or stimulated with 100 nM insulin (Ins) for 20 min at 37°C, fixed, and incubated with anti-HA antibodies in the absence of saponin. Representative images are shown. Scale bar, 60 μm. (B) IRAP-TfR–expressing cells were serum starved for 120 min and treated with DMSO ± 10 μM Lat-B for 60 min. Cells were then either unstimulated (Bas) or stimulated with 100 nM insulin (Ins) for 20 min at 37°C. IRAP-TfR on the PM was visualized by surface labeling with Tf-Alexa-488 at 4°C for 60 min. Representative images are shown. Scale bar, 40 μm. (C) As in A, but HA-GLUT4–expressing cells were grown in 96-well plates, and surface HA-GLUT4 expression under nonpermeabilizing conditions was expressed as a percentage of total HA-GLUT4 determined under permeabilizing conditions. * $p < 0.05$ versus DMSO control insulin (n = 3 experiments).

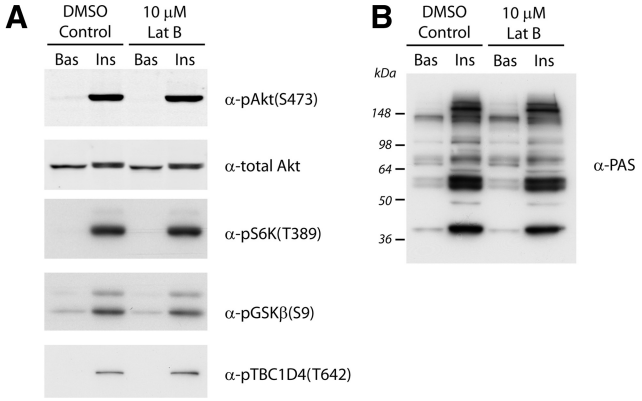

Figure 4. Insulin signaling through Akt/PKB proceeds in the absence of an intact cortical actin network. 3T3-L1 adipocytes were serum-starved for 120 min and treated with DMSO ± 10 μM Lat-B for 60 min. Cells were then either unstimulated (Bas) or stimulated with 100 nM insulin (Ins) for 30 min at 37°C. Whole-cell lysates were immunoblotted with total Akt, pAkt(S473), pS6K(T389), pGSKβ(S9), or pTBC1D4(T642) antibodies (A) or rabbit monoclonal phosho-Akt-substrate (PAS) antibody (B). Representative blots are shown (n = 3 experiments).

described (Govers *et al.*, 2004). Treatment with Lat-B significantly ($p < 0.05$) inhibited the insulin-stimulated appearance of HA-GLUT4 on the cell surface (Figure 3, A and C). We also used an alternative reporter for measuring the trafficking of GLUT4 to the PM to exclude the possibility that Lat-B may have an indirect effect by masking the exposure of the HA epitope. The IRAP-TfR chimera consists of the lumenally exposed transferrin receptor and its transmembrane domain conjugated to the cytosolic domain of the IRAP protein, a known resident of the GLUT4 vesicle. The trafficking of this reporter correlates very well with GLUT4 (Subtil *et al.*, 2000). Surface labeling of the TfR can therefore be assessed using fluorescently labeled transferrin. As seen with HA-GLUT4, treatment of adipocytes with insulin resulted in a dramatic increase in the surface labeling of the transferrin chimera, seen as characteristic rims (Figure 3B). Insulin-stimulated transferrin surface labeling was inhibited by prior treatment of cells with Lat-B (Figure 3B), consistent with observations using HA-GLUT4. Thus, actin remodeling is a requirement for the insulin-stimulated exocytosis of GLUT4.

Insulin Signaling through Akt/PKB Proceeds in the Absence of an Intact Cortical Actin Network

To further investigate the requirement for actin in GLUT4 vesicle exocytosis, we examined the possibility that disruption of cortical actin may impair insulin signaling through Akt/PKB. Indeed, a study by Eyster *et al.* (2005) proposed that cortical actin may act as a scaffold for localized concentrations of signaling complexes in adipocytes. Insulin-stimulated cells with and without Lat-B treatment were examined by Western blot analysis for the phosphorylation events characteristic of insulin signaling (Figure 4). We found no differences in insulin-induced phosphorylation of Akt on Ser473 or phosphorylation of S6 kinase on Thr389 after Lat-B treatment (Figure 4A). Importantly, we consistently observed that phosphorylation of downstream substrates of Akt, including Glycogen synthesis kinase 3 and the RabGAP TBC1D4 was also unaffected by latrunculin treatment (Figure 4A). Furthermore, immunoblotting with a phospho-Akt Substrate (PAS) antibody did not reveal any difference in the insulin-induced phosphorylation profile

after latrunculin treatment (Figure 4B). Although Eyster *et al.* (2005) observed that treatment of adipocytes with Lat-B inhibited the activity of the insulin responsive kinase Akt and its phosphorylation on Ser473, notably, the insulin-induced phosphorylation of substrates downstream of Akt was not examined. Our observations and those of Kanzaki and Pessin (2001) show no significant effect on Akt phosphorylation or downstream signaling, suggesting that insulin induced actin remodeling may play a role in GLUT4 exocytosis that is distal to these signaling events.

Cortical Actin Remodeling Is Not Required for Insulin-induced Transport of GLUT4 Vesicles into the Evanescent Field

The exocytosis of GLUT4 from an intracellular pool to the cell periphery has been shown to involve microtubules and kinesin motor proteins (Semiz *et al.*, 2003) distributed throughout the cell. Chen *et al.* (2008) recently established that microtubular disruption could inhibit a distal step regulating insulin-induced GLUT4 exocytosis, as nocodazole treatment reduced GLUT4 vesicles that could be imaged near the PM in the TIRFM evanescent field. We used TIRF microscopy to assess the role of actin in the insulin-regulated transport of vesicles to the PM in 3T3-L1 adipocytes expressing GLUT4-eGFP (Figure 5). Insulin consistently and reproducibly stimulated the movement of the GLUT4-eGFP reporter toward the PM, resulting in approximately a 3.5-fold increase in GFP fluorescence detected by TIRFM over 20 min (Figure 5A). Surprisingly, treatment of adipocytes with Lat-B had no significant effect on either the kinetics or magnitude of this insulin-stimulated GLUT4 movement response (Figure 5, A and B). These observations were in complete contrast to those seen for Lat-B treatment on insulin-stimulated HA-GLUT4 exocytosis (Figure 3) These data suggest that the insulin-regulated movement of GLUT4 vesicles to the PM is independent of the actin cytoskeleton. Importantly, the insulin-stimulated movement of GLUT4 toward the PM, into the evanescent field, was sensitive to a range of pharmacological inhibitors of insulin signaling. Chelation of intracellular calcium using BAPTA-AM, inhibition of PI3-K by wortmannin or inhibition of Akt using a specific Akti-1/2 inhibitor were found to inhibit both movement of GLUT4-eGFP into the evanescent field (Figure 5, C, E, and G, respectively) and exocytosis of HA-GLUT4 reporter molecules with the PM (Figure 5, D, F, and H, respectively). These data demonstrate that although there is a requirement for intracellular calcium, PI3-K and Akt in the insulin-induced movement of vesicles in the TIRFM evanescent field, there is no significant role for actin. We propose that actin participates in a critical distal regulatory step located within the evanescent field, close to or at the PM.

Cortical Actin Disruption Inhibits IRAP-pHluorin Fluorescence Increase in the Evanescent Field

Using conventional GLUT4 trafficking assays, we have shown that latrunculin treatment inhibits GLUT4 exocytosis. However, GLUT4-eGFP movement into the evanescent field was insensitive to Lat-B. These data suggest that GLUT4 vesicle recruitment or accumulation under the PM is not defective, and therefore one hypothesis is that Lat-B treatment inhibits a more distal step in the exocytosis of GLUT4 such as the final fusion step. To test this hypothesis, we used TIRFM to image 3T3-L1 adipocytes expressing the pH-sensitive IRAP-pHluorin (IRAP-pH) construct (Jiang *et al.*, 2008). IRAP is a transmembrane resident of GLUT4 vesicles (Kupriyanova *et al.*, 2002; Larance *et al.*, 2005) and has been used in a number of studies to monitor GLUT4 trafficking (Garza and Birnbaum, 2000; Subtil *et al.*, 2000). The pH-sensitive GFP derivative, pHluorin, has also been used in many exocytotic systems to monitor the fusion of acidic vesicles/granules with the PM (Miesenbock *et al.*, 1998; Tsuboi and Rutter, 2003). IRAP-pH has been constructed placing pHluorin on the COOH-terminus of the molecule, within the lumen of a GLUT4 vesicle (Jiang *et al.*, 2008). In the case of IRAP-pH in adipocytes, vesicles can be visualized by TIRFM entering the evanescent field, and after fusion exhibit dramatic increase in fluorescence upon exposure to the extracellular environment (Figure 6; Supplementary Material, Movie 2). Thus the IRAP-pH construct is ideal for the study of GLUT4 vesicle fusion. Using this approach, individual cells were imaged by TIRFM before and then after 30 min of insulin stimulation (100 nM). In these cells membrane-associated fluorescence was seen to increase by 4.5-fold over basal levels, consistent with an increase of IRAP-pH–containing vesicles in the evanescent field and the insulin-stimulated fusion of vesicles with the PM (Figure 6A). Pretreatment of cells with 10 μM Lat-B resulted in a significant inhibition (~40%) in insulin-stimulated IRAP-pH membrane fluorescence (Figure 6A). This observation was further confirmed using high-frequency long-term TIRF microscopy on single cells to examine the IRAP-pH fluorescence over the full insulin time course. Insulin stimulation resulted in a rapid increase in fluorescence over 20 min of high-frequency imaging (Figure 6B; Supplementary Material, Movie 2). Again, Lat-B pretreatment significantly reduced ($p < 0.001$) this effect. Both the rate and magnitude of the fluorescence increase imaged by TIRFM was significantly inhibited by treatment with Lat-B (Figure 6, B and C). Thus we propose that in cells treated with insulin and Lat-B, whereas GLUT4 vesicles are able to enter the evanescent field close to the PM (Figure 5A), the fusion event exposing lumenal contents including the pHluorin molecule is inhibited.

Cortical Actin Remodeling Facilitates the Fusion of GLUT4 Vesicles at the PM

To more accurately examine whether the actual fusion event was inhibited in Lat-B–treated cells, we sought to quantify the number of fusion events in insulin-stimulated cells with and without Lat-B. Individual fusion events imaged via IRAP-pH consists of a series of characteristic steps as a vesicle first becomes visible within the evanescent field (Figure 7A, time 0 s) and subsequently fuses (Figure 7A, time 0.1 s), resulting in lateral diffusion of the fluorescence into the PM (Supplementary Material, Movie 3). The fluorescence profile of this event is shown in Figure 7B and is consistent with that observed by others (Jiang *et al.*, 2008). To accurately quantify the number of fusion events, we developed an automated fusion detection algorithm known as TIRF Explorer to identify this characteristic profile in high-frequency long-term TIRF experiments. In insulin-stimulated cells TIRF Explorer identified a rapid increase in the number of fusion events upon addition of the stimulus (Figure 7C). The number of identified events correlated well with the increase in cell membrane fluorescence seen in these experiments (Figure 7C). Insulin stimulation increased the rate of fusion fivefold over the basal state ($p < 0.01$; Figure 7E). In contrast, the number of fusion events identified in Lat-B–treated cells was significantly reduced ($p < 0.01$; Figure 7, D and E), confirming that actin remodeling is required for the efficient fusion of GLUT4 vesicles with the PM.

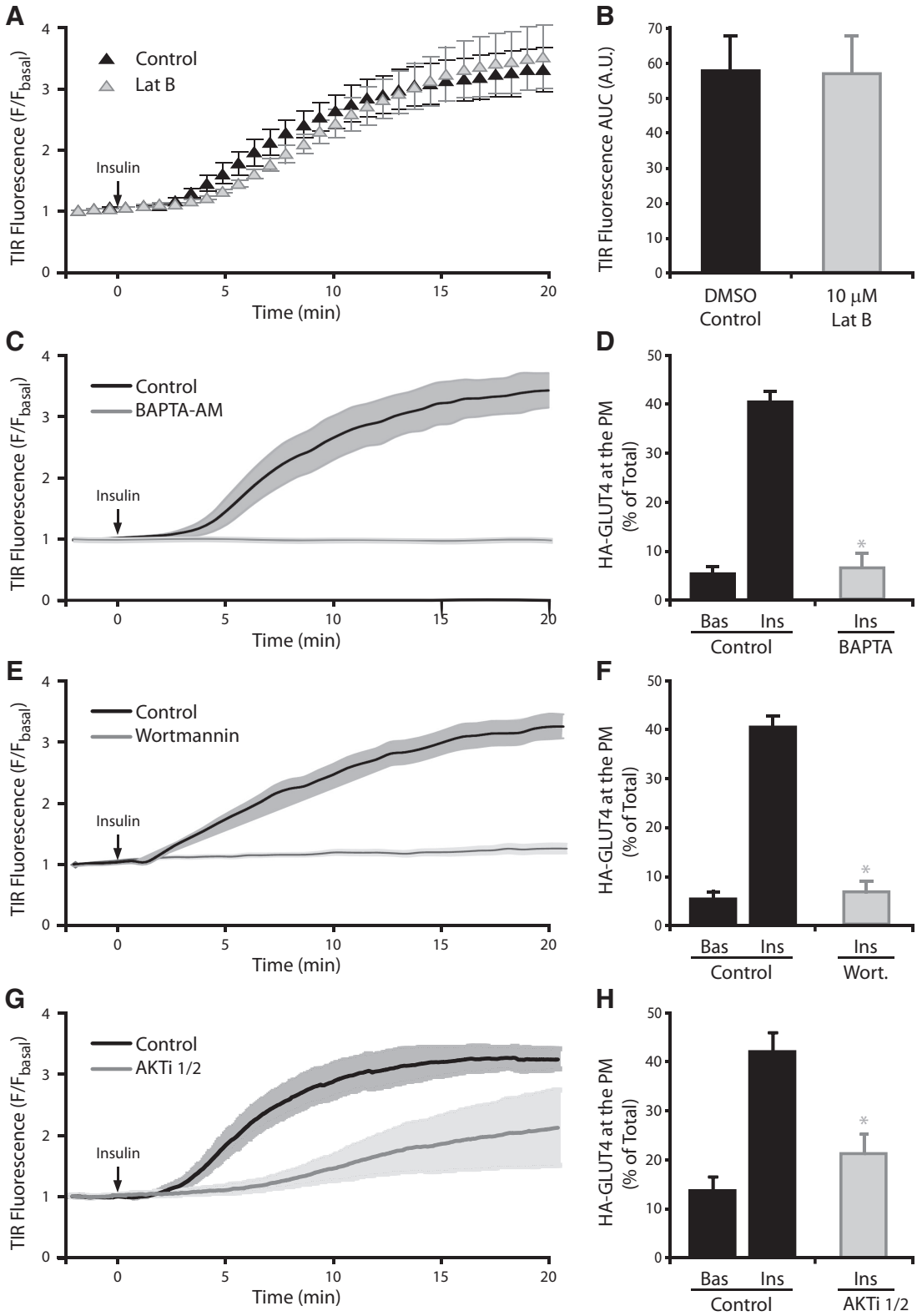

Figure 5. Cortical actin remodeling is not required for insulin-induced transport of GLUT4 vesicles into the evanescent field. 3T3-L1 adipocytes expressing GLUT4-eGFP were serum starved for 120 min and treated with DMSO ± 10 μM Lat-B for 60 min. Time course of insulin-induced GLUT4-eGFP fluorescence increase in the evanescent field for DMSO and Lat-B treatments (A) and the area under the curve (B) are shown. Data are mean ± SEM (n = 3 experiments); time-course of insulin-induced GLUT4-eGFP fluorescence increase in the evanescent field for DMSO control and 50 μM BAPTA-AM (C), 100 nM wortmannin (E), or 10 μM Akti-1/2 inhibitor (G) treatments. Data are mean ± SEM of 2–3 independent experiments; HA-GLUT4–expressing adipocytes grown in 96-well plates were serum-starved for 2 h and treated with DMSO control and 50 μM BAPTA-AM (D), 100 nM wortmannin (F), or 10 μM Akti-1/2 inhibitor (H) treatments. Cells were then either unstimulated (Bas) or stimulated with 100 nM insulin (Ins) for 20 min at 37°C. The amount of HA-GLUT4 on the cell surface (nonpermeabilized cells) was expressed as a percentage of total HA-GLUT4 determined under permeabilizing conditions. * $p < 0.05$ versus DMSO control insulin (n = 3 experiments).

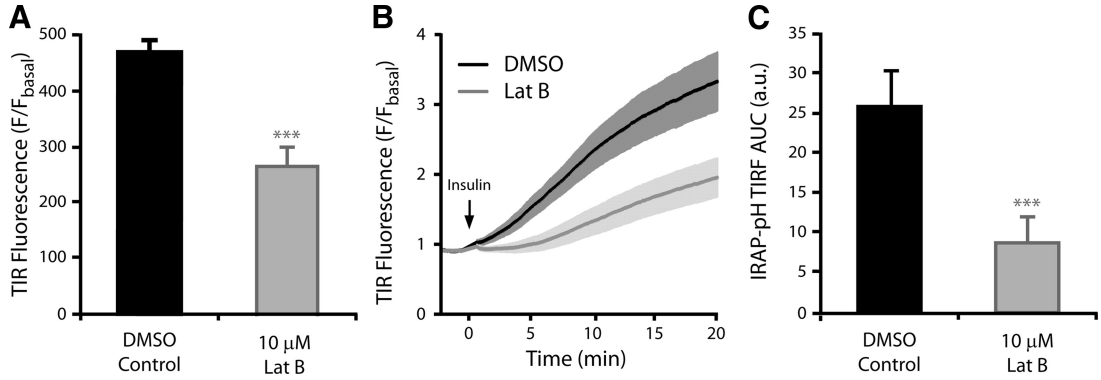

Figure 6. Cortical actin disruption inhibits IRAP-pHluorin fluorescence increase in the evanescent field. 3T3-L1 adipocytes expressing IRAP-pH were serum-starved for 120 min and treated with DMSO ± 10 μM Lat-B for 60 min. (A) Static TIRFM images were taken before and after 30 min of insulin stimulation. Data are mean ± SEM of six experiments (10 cells/experiment). IRAP-pH expressing 3T3L1s were imaged by high-frequency TIRFM (~10 Hz) for 2 min before stimulation with 100 nM insulin (at t = 0) and then imaged for a further 20 min. The mean time course of DMSO and Lat-B treatments (B) and the area under the curve (C) are shown. Data are mean ± SEM (n = 8). *** $p < 0.001$ versus DMSO control.

IRAP-pH–containing Vesicles Accumulate under the PM after Cortical Actin Disruption

In Lat-B–treated cells very few vesicles undergo fusion, and the consequence of this is apparent when we performed a detailed analysis of IRAP-pH vesicle behavior under these conditions. After insulin stimulation vesicles appear in the evanescent field and display a stationary or restricted behavior. Some restricted vesicles, unable to fuse, ultimately leave the evanescent field again. An example of this behavior is shown in Figure 8A, and the fluorescence profile of this event is shown in Figure 8B. Unlike fusion, there is a small increase in fluorescence that is maintained until the vesicle leaves the evanescent field. In addition, some vesicles appear to remain trapped at the membrane. This can be seen as an increase in the number of stationary vesicles in the evanescent field after insulin stimulation (Figure 8D), an in-

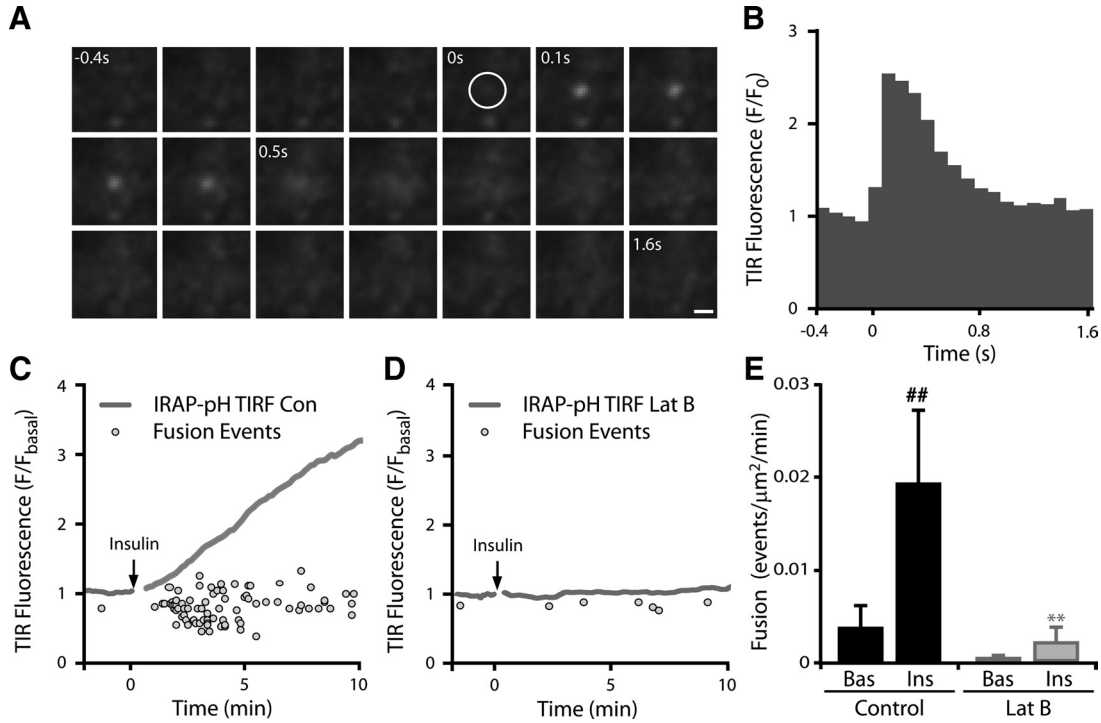

Figure 7. Cortical actin remodeling facilitates the fusion of GLUT4 vesicles at the PM. Individual fusion events can be visualized by TIRFM imaging. (A) A time series of a representative IRAP-pH containing vesicle undergoing fusion is shown imaged by high-frequency TIRFM (~10 Hz). The vesicle, first visible in frame 5 (circle), fuses with the PM at frame 6, followed by lateral diffusion into the PM. Scale bar, 1 μm. (B) The fluorescence profile of the event is shown. Adipocytes expressing IRAP-pH were serum-starved for 120 min and treated with DMSO ± 10 μM Lat-B for 60 min. A fluorescence trace and individual fusion events identified using TIRF explorer are shown for representative cells treated with DMSO (C) and Lat-B (D). Average rate of fusion in cells pretreated for 1 h with DMSO or 10 μM Lat-B before and after insulin stimulation (H) is shown. Data are mean ± SEM (n = 3). ** $p < 0.01$ versus DMSO control insulin, ## $p < 0.01$ versus DMSO control basal.

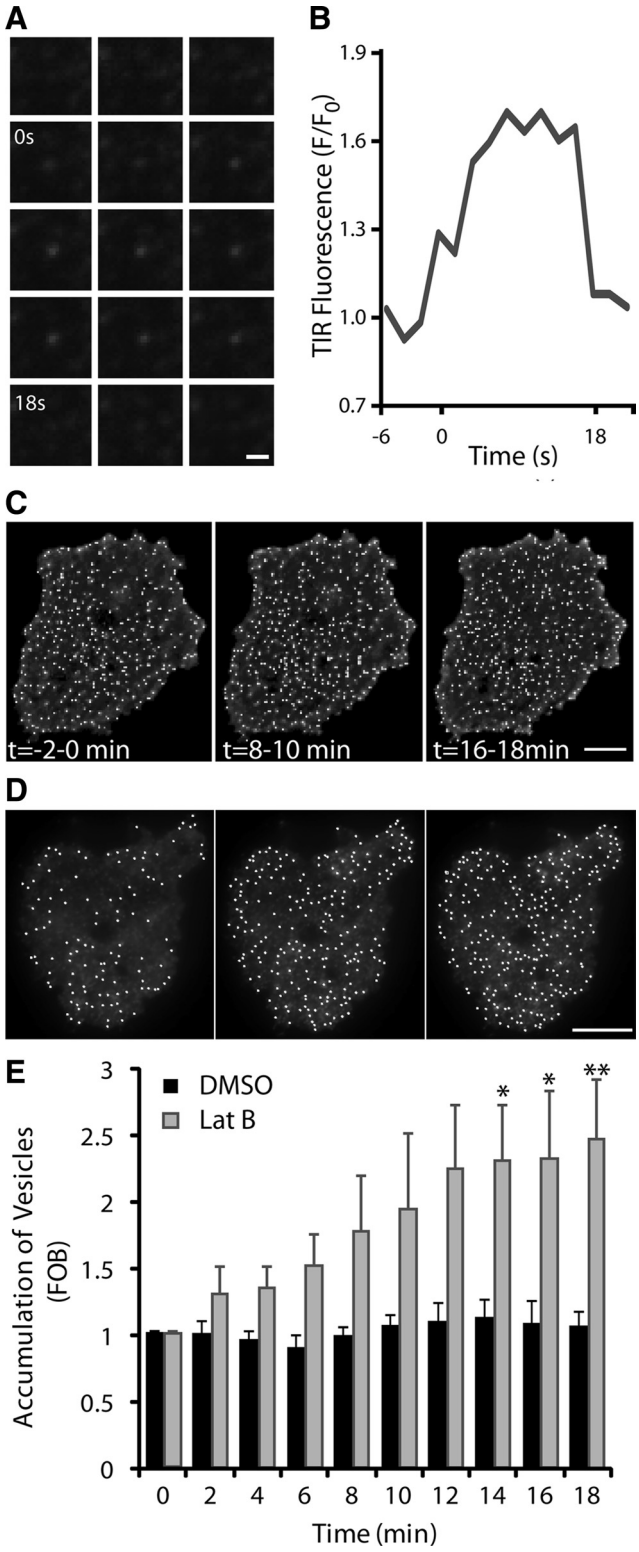

Figure 8. IRAP-pH–containing vesicles accumulate under the PM after cortical actin disruption. (A) Representative behavior of IRAP-pH vesicles in the evanescent field after insulin stimulation in the presence of Lat-B. A vesicle enters the evanescent field at time 0 and remains in a restricted or "tethered" state for 18 s before leaving. (B) Fluorescence profile of panel A. Time course of vesicle numbers in the evanescent field after insulin stimulation. Images are average projections of basal (−2–0 min), 6–8 min, and 16–18 min after insulin. Spots representing GLUT4 vesicles were identified by Imaris and are shown overlayed, control cell (C) and Lat-B–treated cells (D). Although total numbers vary between all cells irrespective of treatment, accumulation is only seen in Lat-B–treated cells (D). (E) Quantification of vesicle accumulation in the evanescent field. Data are mean ± SEM (n = 3).

crease that does not occur in the absence of Lat-B (Figure 8C). The number of IRAP-pH vesicles in the evanescent field was shown to increase 2.3-fold after insulin treatment (Figure 8E). These observations are consistent with our hypothesis that actin remodeling is required *after* insulin-stimulated vesicle movement to a near PM location within the evanescent field. This actin remodeling is required to allow the final step in the exocytotic process: fusion of the GLUT4 vesicle with the PM. This represents a novel function for actin proximal to membrane bilayer fusion, presumably in association with the tethering and docking process required for GLUT4 vesicle exocytosis.

DISCUSSION

In this study we describe a previously unidentified role for cortical actin rearrangement at one of the most distal steps in the process of insulin-dependent GLUT4 accumulation at the PM in adipocytes. Filamentous actin is found predominantly at the cell periphery in the adipocyte, consistent with it being involved in late stages of vesicle trafficking and fusion. Insulin treatment results in significant remodeling of cortical actin in adipocytes. Treatment of adipocytes with Lat-B disrupts filamentous actin remodeling and inhibits insertion of GLUT4 into the PM. Given that both upstream insulin signaling and the microtubule network appear to remain intact under these conditions, this observation suggests that actin remodeling is an important component of the final stages of GLUT4 trafficking. Surprisingly, using TIRF microscopy, although fusion of GLUT4 vesicles with the PM was seen to be inhibited by Lat-B actin disruption, the insulin-dependent accumulation of GLUT4-eGFP fluorescence in the evanescent field was unperturbed. This suggests that insulin stimulates the movement and accumulation of GLUT4 vesicles close to the PM, possibly involving a direct interaction between these two organelles, and this step does not require cortical actin rearrangement. This step precedes the fusion event. Actin rearrangement is required to permit the final fusion of GLUT4-containing vesicles with the PM and thus the insertion of GLUT4 into the PM. Hence, these data support a model where the insulin-dependent trafficking of GLUT4 to the PM involves at least two regulated steps, with the latter involving actin rearrangement at or close to the process of vesicle fusion.

Using IRAP-pH protein as a reporter of GLUT4 vesicle fusion, we show that inhibition of actin remodeling specifically inhibited the rate at which GLUT4 vesicles fuse with the PM. Thus, by inhibiting actin remodeling we have been able to arrest the majority of vesicles, presumably in a tethered/docked but nonfused state. Actin may be involved in a step immediately before fusion or in the fusion process itself. Indeed, actin has been previously implicated in membrane fusion. In yeast, for example, there is evidence that actin remodeling regulates the homotypic fusion of vacuoles (Eitzen *et al.*, 2002). Eitzen and colleagues used an in vitro vacuole fusion assay to discriminate a role for actin in either the priming, docking, or fusion of vacuoles. Actin was found to be enriched at the vertices of docked granules and addition of Lat-B at different stages of this in vitro fusion reaction

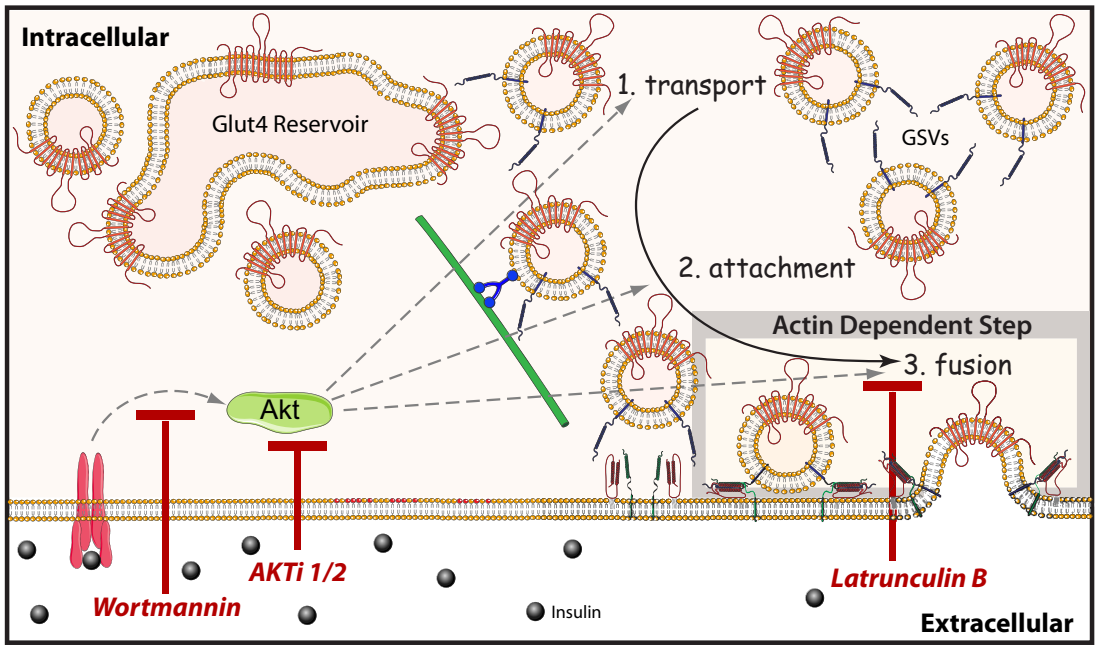

Figure 9. Cortical actin remodeling controls a distal GLUT4-trafficking event. Insulin initiates the translocation of GLUT4 vesicles along microtubules from an intracellular storage compartment to the PM. We propose Akt functions at multiple steps in the process, to regulate the transport (1), attachment (2), and fusion (3) of GLUT4 vesicles. Inhibiting Akt function upstream impairs vesicle attachment and fusion at the PM. In contrast, actin polymerization specifically regulates this process downstream of vesicle attachment, at a step that may directly drive the incorporation of GLUT4 into the PM.

demonstrated a specific role for actin in the terminal fusion and bilayer mixing step. In contrast, also using an in vitro assay, Koumanov *et al.* (2005) demonstrated that Lat-B had no effect on insulin-stimulated GLUT4 vesicle fusion. However, these authors do highlight that their in vitro system specifically allows the fusion step to be studied in an environment isolated from any involvement of the cytoskeleton.

The handover from GLUT4 vesicle docking to fusion may be aided by interactions between SNARE proteins and actin. In fact there is a growing body of evidence for a functional interaction between actin and the SNARE docking machinery. A study investigating the composition of the fusion pore in secretory cells demonstrated that *t*-SNAREs, actin, and fodrin proteins were major constituents of these pores (Jena *et al.*, 2003). Interestingly, previous studies have shown that the *t*-SNAREs that regulate GLUT4 docking and fusion at the PM, SNAP23, and Syntaxin4 localize to actin-rich areas in insulin-responsive cells (Tong *et al.*, 2001). More recently, Jewell *et al.* (2008) have reported a direct interaction between actin and Syntaxin4. This interaction was observed in vivo and was disrupted by treatment of cells with Lat B. In addition, another study showed that the actin-binding protein fodrin, binds to Syntaxin4 in rat adipocytes and that insulin enhances this interaction (Liu *et al.*, 2006). Disruption of filamentous actin with latrunculin A inhibited this interaction and in agreement with our studies, led to a block in GLUT4 appearance on the PM. Interestingly, treatment of the adipocytes with cytochalasin D, which preferentially affects short actin filaments had no effect on GLUT4 trafficking. The authors proposed that insulin-induced fodrin remodeling regulates the fusion of GLUT4 vesicles with the PM.

It has previously been suggested that actin controls the assembly of the Akt/PKB signaling pathway in adipocytes (Eyster *et al.*, 2005). In our studies Lat-B treatments induced major inhibition of actin remodeling as well as GLUT4 trafficking, but did not lead to any significant change in the phosphorylation of Akt/PKB or downstream substrates, as detected by Western blot analysis. These data do not preclude the possibility of a small pool of Akt/PKB being actin-remodeling dependent; however, they do suggest that a site of Lat-B "sensitivity" for insulin-stimulated GLUT4 translocation would appear to be downstream of major Akt/PKB phosphorylation events. Although we have not interrogated the molecules that control actin remodeling in adipocytes, we feel that this step is likely to involve Akt/PKB. Activation of Akt alone is sufficient to stimulate GLUT4 trafficking and fusion with the PM in a manner that is indistinguishable from that observed with insulin (Eyster *et al.*, 2005; Ng *et al.*, 2008) and indeed, Akt activity has been shown to be required at the PM to control GLUT4 fusion (Koumanov *et al.*, 2005). Despite these observations, it has also been suggested that insulin signaling through Akt regulates GLUT4 entry into the evanescent field, whereas an Akt-independent mechanism regulates vesicle fusion (Gonzalez and McGraw, 2006). Inhibiting Akt function is difficult to interpret as blocking an upstream process will inevitably have downstream consequences. Inhibiting the movement of vesicles along microtubules, for example, will lead to observed reduction of vesicle docking and fusion. We suggest that Akt plays roles at multiple steps, including regulating the recruitment of vesicles into the evanescent field as well as their subsequent docking and fusion.

On the basis of the current study as well as previously published work, we propose the following model (Figure 9). It should be noted that the core features of this model are based on the use of TIRFM, which is proving to be invaluable tool to resolve key steps in this process. Thus far this has allowed the identification of three major steps in the process that are morphologically distinguished using this technique: 1) transport or movement of vesicles into the TIRF zone; 2) attachment, recognized as stationary vesicles

but not fused; and 3) fusion, distinguishable using IRAP-pH, by a sharp increase in vesicle fluorescence intensity and subsequent lateral diffusion of this fluorescence with the PM. It is unclear to us at the present time whether attachment defines a single step or more because in other exocytotic systems this involves several processes referred to as tethering, priming, and docking (Verhage and Sorensen, 2008). Attachment may well represent multiple processes, but as yet we are unable to resolve these. Transport likely involves microtubules, as shown by others (Olson *et al.*, 2001) and indeed disruption of microtubules blocks movement into the evanescent field (Chen *et al.*, 2008). Similarly, inhibition of Akt/PKB function by either wortmannin treatment or a specific Akt inhibitor also inhibits the accumulation of vesicles in the evanescent field. This could mean that Akt is involved either in the transport step or in the attachment step itself. The studies described here represent a major advance because they have enabled us for the first time to resolve the late stages of GLUT4 trafficking. Thus, in the absence of actin remodeling we propose that the microtubule-dependent transport step still occurs and that these vesicles either remain attached at the minus end of the tubule or disengage from the microtubule and engage in a separate attachment step that precedes actin function. A major focus of future work will be to dissect the step at which SNAREs function and it will be intriguing to determine if this is the same step regulated by actin.

ACKNOWLEDGMENTS

We thank Dr. Tao Xu for the IRAP-pHluorin and GLUT4-eGFP plasmids, Dr. Timothy McGraw for the VpTfR plasmid, and Dr. Cordula Hohnen-Behrens for technical assistance. This work was supported by grants from the National Health and Medical Research Council (NHMRC) of Australia and Diabetes Australia to D.E.J and W.E.H. D.E.J is an NHMRC Senior Principal Research Fellow.

REFERENCES

Axelrod, D. (2008). Total internal reflection fluorescence microscopy. Biophysical tools for biologists. In Vivo Techniques *89*, 169–221.

Bai, L., Wang, Y., Fan, J., Chen, Y., Ji, W., Qu, A., Xu, P., James, D. E., and Xu, T. (2007). Dissecting multiple steps of GLUT4 trafficking and identifying the sites of insulin action. Cell Metab. *5*, 47–57.

Bao, Y., Lopez, J. A., James, D. E., and Hunziker, W. (2008). Snapin interacts with the Exo70 subunit of the exocyst and modulates GLUT4 trafficking. J. Biol. Chem. *283*, 324–331.

Bose, A., Robida, S., Furcinitti, P. S., Chawla, A., Fogarty, K., Corvera, S., and Czech, M. P. (2004). Unconventional myosin Myo1c promotes membrane fusion in a regulated exocytic pathway. Mol. Cell. Biol. *24*, 5447–5458.

Burchfield, J. G., Lopez, J. A., Mele, K., Vallotton, P., James, D. E., and Hughes, W. E. (2009). Exocytotic vesicle behaviour assessed by total internal reflection fluorescence microscopy. *Traffic* (*in press*).

Chen, Y., Wang, Y., Ji, W., Xu, P. Y., and Xu, T. (2008). A pre-docking role for microtubules in insulin-stimulated glucose transporter 4 translocation. FEBS J. *275*, 705–712.

Eitzen, G., Wang, L., Thorngren, N., and Wickner, W. (2002). Remodeling of organelle-bound actin is required for yeast vacuole fusion. J. Cell Biol. *158*, 669–679.

Eyster, C. A., Duggins, Q. S., and Olson, A. L. (2005). Expression of constitutively active Akt/protein kinase B signals GLUT4 translocation in the absence of an intact actin cytoskeleton. J. Biol. Chem. *280*, 17978–17985.

Falasca, M., Hughes, W. E., Dominguez, V., Sala, G., Fostira, F., Fang, M. Q., Cazzolli, R., Shepherd, P. R., James, D. E., and Maffucci, T. (2007). The role of phosphoinositide 3-kinase C2 alpha in insulin signaling. J. Biol. Chem. *282*, 28226–28236.

Fletcher, L. M., Welsh, G. I., Oatey, P. B., and Tavare, J. M. (2001). Role for the microtubule cytoskeleton in GLUT4 vesicle trafficking and in the regulation of insulin-stimulated glucose uptake. Biochem. J. *353*, 735–735.

Garza, L. A., and Birnbaum, M. J. (2000). Insulin-responsive aminopeptidase trafficking in 3T3–L1 adipocytes. J. Biol. Chem. *275*, 2560–2567.

Gonzalez, E., and McGraw, T. E. (2006). Insulin signaling diverges into Akt-dependent and -independent signals to regulate the recruitment/docking and the fusion of GLUT4 vesicles to the plasma membrane. Mol. Biol. Cell *17*, 4484–4493.

Govers, R., Coster, A.C.F., and James, D. E. (2004). Insulin increases cell surface GLUT4 levels by dose dependently discharging GLUT4 into a cell surface recycling pathway. Mol. Cell. Biol. *24*, 6456–6466.

Huang, S. H., Lifshitz, L. M., Jones, C., Bellve, K. D., Standley, C., Fonseca, S., Corvera, S., Fogarty, K. E., and Czech, M. P. (2007). Insulin stimulates membrane fusion and GLUT4 accumulation in clathrin coats on adipocyte plasma membranes. Mol. Cell. Biol. *27*, 3456–3469.

Inoue, M., Chang, L., Hwang, J., Chiang, S. H., and Saltiel, A. R. (2003). The exocyst complex is required for targeting of Glut4 to the plasma membrane by insulin. Nature *422*, 629–633.

Jena, B. P., Cho, S. J., Jeremic, A., Stromer, M. H., and Abu-Hamdah, R. (2003). Structure and composition of the fusion pore. Biophys. J. *84*, 1337–1343.

Jewell, J. L., Luo, W., Oh, E., Wang, Z., and Thurmond, D. C. (2008). Filamentous actin regulates insulin exocytosis through direct interaction with Syntaxin 4. J. Biol. Chem. *283*, 10716–10726.

Jiang, L., Fan, J. M., Bai, L., Wang, Y., Chen, Y., Yang, L., Chen, L. Y., and Xu, T. (2008). Direct quantification of fusion rate reveals a distal role for AS160 in insulin-stimulated fusion of GLUT4 storage vesicles. J. Biol. Chem. *283*, 8508–8516.

Jiang, Z. Y., Chawla, A., Bose, A., Way, M., and Czech, M. P. (2002). A phosphatidylinositol 3-kinase-independent insulin signaling pathway to N-WASP/Arp2/3/F-actin required for GLUT4 glucose transporter recycling. J. Biol. Chem. *277*, 509–515.

Kanzaki, M., and Pessin, J. E. (2001). Insulin-stimulated GLUT4 translocation in adipocytes is dependent upon cortical actin remodeling. J. Biol. Chem. *276*, 42436–42444.

Kanzaki, M., Watson, R. T., Hou, J. C., Stamnes, M., Saltiel, A. R., and Pessin, J. E. (2002). Small GTP-binding protein TC10 differentially regulates two distinct populations of filamentous actin in 3T3L1 adipocytes. Mol. Biol. Cell *13*, 2334–2346.

Koumanov, F., Jin, B., Yang, J., and Holman, G. D. (2005). Insulin signaling meets vesicle traffic of GLUT4 at a plasma-membrane-activated fusion step. Cell Metab. *2*, 179–189.

Kupriyanova, T. A., Kandror, V., and Kandror, K. V. (2002). Isolation and characterization of the two major intracellular Glut4 storage compartments. J. Biol. Chem. *277*, 9133–9138.

Larance, M., Ramm, G., and James, D. E. (2008). The GLUT4 code. Mol. Endocrinol. *22*, 226–233.

Larance, M., *et al.* (2005). Characterization of the role of the Rab GTPase-activating protein AS160 in insulin-regulated GLUT4 trafficking. J. Biol. Chem. *280*, 37803–37813.

Latham, C. F., *et al.* (2006). Molecular dissection of the Munc18c/syntaxin4 interaction: Implications for regulation of membrane trafficking. Traffic *7*, 1408–1419.

Li, C. H., Bai, L., Li, D. D., Xia, S., and Xu, T. (2004). Dynamic tracking and mobility analysis of single GLUT4 storage vesicle in live 3T3–L1 cells. Cell Res. *14*, 480–486.

Liu, L. B., Jedrychowski, M. P., Gygi, S. P., and Pilch, P. F. (2006). Role of insulin-dependent cortical fodrin/spectrin remodeling in glucose transporter 4 translocation in rat adipocytes. Mol. Biol. Cell *17*, 4249–4256.

Lizunov, V. A., Matsumoto, H., Zimmerberg, J., Cushman, S. W., and Frolov, V. A. (2005). Insulin stimulates the halting, tethering, and fusion of mobile GLUT4 vesicles in rat adipose cells. J. Cell Biol. *169*, 481–489.

Mele, K., Coster, A., Burchfield, J. G., Lopez, J., James, D. E., Hughes, W. E., and Valotton, P. (2009). Automatic identification of fusion events in TIRF microscopy image sequences. [conference paper] In: ICCV09 1st Workshop on Video-oriented Object and Event Classification (VOEC'09), Kyoto, Japan, 28 September 2009.

Miesenbock, G., De Angelis, D. A., and Rothman, J. E. (1998). Visualizing secretion and synaptic transmission with pH-sensitive green fluorescent proteins. Nature *394*, 192–195.

Morton, W. M., Ayscough, K. R., and McLaughlin, P. J. (2000). Latrunculin alters the actin-monomer subunit interface to prevent polymerization. Nat. Cell Biol. *2*, 376–378.

Ng, Y., Ramm, G., Lopez, J. A., and James, D. E. (2008). Rapid activation of Akt2 is sufficient to stimulate GLUT4 translocation in 3T3–L1 adipocytes. Cell Metab. *7*, 348–356.

Nobes, C. D., and Hall, A. (1995). Rho, rac, and cdc42 GTPases regulate the assembly of multimolecular focal complexes associated with actin stress fibers, lamellipodia, and filopodia. Cell *81*, 53–62.

Olson, A. L., Trumbly, A. R., and Gibson, G. V. (2001). Insulin-mediated GLUT4 translocation is dependent on the microtubule network. J. Biol. Chem. *276*, 10706–10714.

Omata, W., Shibata, H., Li, L., Takata, K., and Kojima, I. (2000). Actin filaments play a critical role in insulin-induced exocytotic recruitment but not in endocytosis of GLUT4 in isolated rat adipocytes. Biochem. J. 346(Pt 2), 321–328.

Patki, V., Buxton, J., Chawla, A., Lifshitz, L., Fogarty, K., Carrington, W., Tuft, R., and Corvera, S. (2001). Insulin action on GLUT4 traffic visualized in single 3T3–L1 adipocytes by using ultra-fast microscopy. Mol. Biol. Cell *12*, 129–141.

Semiz, S., Park, J. G., Nicoloro, S. M., Furcinitti, P., Zhang, C., Chawla, A., Leszyk, J., and Czech, M. P. (2003). Conventional kinesin KIF5B mediates insulin-stimulated GLUT4 movements on microtubules. EMBO J. *22*, 2387–2399.

Shewan, A. M., van Dam, E. M., Martin, S., Luen, T. B., Hong, W. J., Bryant, N. J., and James, D. E. (2003). GLUT4 recycles via a trans-Golgi network (TGN) subdomain enriched in Syntaxins 6 and 16 but not TGN38, involvement of an acidic targeting motif. Mol. Biol. Cell *14*, 973–986.

Slot, J. W., Geuze, H. J., Gigengack, S., Lienhard, G. E., and James, D. E. (1991). Immuno-localization of the insulin regulatable glucose transporter in brown adipose-tissue of the rat. J. Cell Biol. *113*, 123–135.

Spector, I., Shochet, N. R., Kashman, Y., and Groweiss, A. (1983). Latrunculins—novel marine toxins that disrupt microfilament organization in cultured-cells. Science *219*, 493–495.

Stockli, J., Davey, J. R., Hohnen-Behrens, C., Xu, A., James, D. E., and Ramm, G. (2008). Regulation of glucose transporter 4 translocation by the Rab guanosine triphosphatase-activating protein AS160/TBC1D4, role of phosphorylation and membrane association. Mol. Endocrinol. *22*, 2703–2715.

Subtil, A., Lampson, M. A., Keller, S. R., and McGraw, T. E. (2000). Characterization of the insulin-regulated endocytic recycling mechanism in 3T3–L1 adipocytes using a novel reporter molecule. J. Biol. Chem. *275*, 4787–4795.

Taniguchi, C. M., Emanuelli, B., and Kahn, C. R. (2006). Critical nodes in signalling pathways: insights into insulin action. Nat. Rev. Mol. Cell. Biol. *7*, 85–96.

Tong, P., Khayat, Z. A., Huang, C., Patel, N., Ueyama, A., and Klip, A. (2001). Insulin-induced cortical actin remodeling promotes GLUT4 insertion at muscle cell membrane ruffles. J. Clin. Inv. *108*, 371–381.

Tsuboi, T., and Rutter, G. A. (2003). Multiple forms of "kiss-and-run" exocytosis revealed by evanescent wave microscopy. Curr. Biol. *13*, 563–567.

Verhage, M., and Sorensen, J. B. (2008). Vesicle docking in regulated exocytosis. Traffic *9*, 1414–1424.

Yip, M. F., Ramm, G., Larance, M., Hoehn, K. L., Wagner, M. C., Guilhaus, M., and James, D. E. (2008). CaMKII-mediated phosphorylation of the myosin motor Myolc is required for insulin-stimulated GLUT4 translocation in adipocytes. Cell Metab. *8*, 384–398.

Zaid, H., Antonescu, C. N., Randhawa, V. K., and Klip, A. (2008). Insulin action on glucose transporters through molecular switches, tracks and tethers. Biochem. J. *413*, 201–215.